A Velocity Coupling Model for High Frequency Instabilities

F. Richecoeur, S. Ducruix and S. Candel
Ecole Centrale Paris, EM2C Laboratory, CNRS
92295 Chatenay-Malabry, France

Abstract

The modeling of liquid rocket high frequency combustion instabilities raises many fundamental questions and it has important practical applications. The modeling question is here reconsidered by revisiting some of the most significant early experiments and by making use of more recent experimental data. Streak films obtained in the early experiments are used to characterize the space-time evolution of heat release in the chamber. These data are combined with recent observations derived from a multiple injector combustor experiments to extract a model for the nonsteady heat release. Based on these experimental observations, a velocity coupling mechanism is devised to show how acoustic velocity fluctuations can drive heat release fluctuations. These may in turn constitute acoustic sources feeding energy into the chamber eigenmodes. In its present form the model involves the transverse velocity delayed by a time τ and the sign of the transverse velocity gradient. For suitable values of the delay τ the heat release and pressure may be in phase and under these circumstances the Rayleigh criterion is satisfied and the acoustic perturbation is amplified. It is shown that this is effectively the case by projecting the pressure field on the normal modes of the system and determining the evolution of the modal amplitude.

1. Introduction

High frequency combustion instabilities constitute a central problem in rocket engine design. An important research effort has been made to obtain a fundamental understanding of the processes driving these instabilities and eventually leading to some spectacular failures.[2,3,6] Models of high frequency instabilities have been developed over many years of research. The most common descriptions are based on the sensitive time lag concept devised about 50 years ago.[1] This has been based on experimental data from early experiments carried out on test engines and on intermediate scale systems. Information was also gathered from some smaller scale experiments but the instrumentation and data acquisition were quite limited. It is therefore timely to reconsider the problem by first revisiting some of the earlier experiments and in particular those of Tischler and Male[5] and by making use of the more recent experimental data obtained in Ref.4.

The recent tests were carried out in a multiple injector combustor (MIC) with three injection elements operating at 1 MPa.[4] The set up comprised a rotating toothed wheel which was used to periodically block an auxialiary nozzle and induce a transverse mode in the system. A wide range of parameters has been explored to determine the mechanisms and key parameters governing the development of combustion oscillations. When modulated at the first transverse eigenfrequency, it was found that strong interactions could be induced between combustion and pressure fluctuations. Systematic experiments were carried out by varying the methane injection velocity and temperature. These variations induced important modifications in the flame structure and dynamics. Low injection velocity led to long flames which were the most receptive to external modulation. Coherence between the pressure and heat release fluctuations occured when the level of oscillation was high. Photo-multipliers indicate that the most intense emission area in the chamber oscillates transversally at the modulation frequency. It was shown that the heat release fluctuations in the upper and lower parts of the chamber were in phase with the pressure signals detected at the upper and lower walls respectively. These two sets of signals were out of phase by 180°.

One may infer that the perturbed heat release field corresponding to this data could be the result of a velocity coupling. This possibility is here specifically considered in what follows. The objective is to see how acoustic velocity fluctuations could drive heat release fluctuations. These perturbations could in turn become acoustic sources feeding energy to a transverse pressure mode. The model is based on data obtained on the multiple injector combustor experiments and specifically on the phase relations established in the low pressure tests. The model also relies on results from earlier investigations of high frequency instabilities in liquid rocket engines (LRE). In the early days, many visualizations were

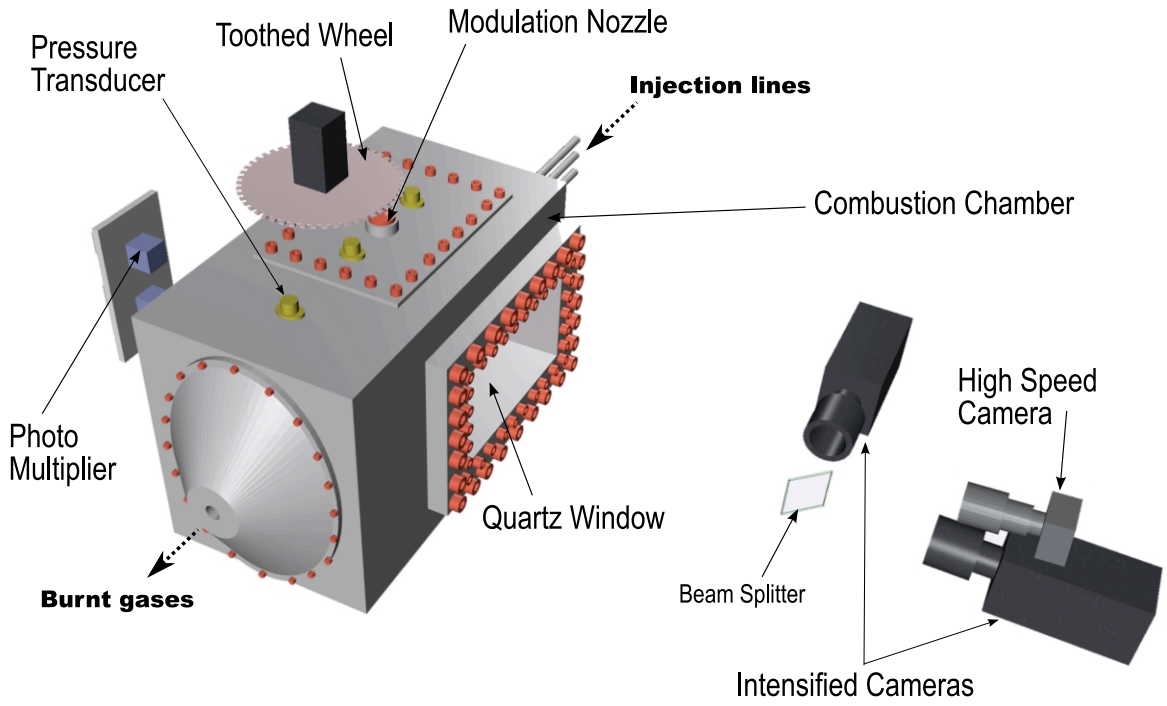

Figure 1: Schematic view of MASCOTTE combustion chamber with the diagnostic set up for the hot fire tests.

based on high speed films recorded with a transverse slit. These can be used to characterize the space-time evolution of heat release in the chamber. These visualizations are revisited and reinterpreted to extract a model for the nonsteady heat release. In its present form, the model involves the transverse velocity delayed by a time τ and the sign of the transverse velocity gradient.

Considering a rectangular chamber geometry similar to that of the MIC, it is shown that the resulting heat release distribution can be subdivided in two parts separated by the symmetry axis. When the heat release fluctuation is positive in the upper part of the chamber, it is negative in its lower part. This configuration is reversed after one half period. This corresponds to what is observed experimentally. The heat release distribution takes a shape which has some similarity with that of the pressure associated with the first transverse mode. For suitable values of the delay τ the heat release and pressure may be in phase. The Rayleigh criterion is satisfied and the acoustic perturbation is amplified. It is shown that this is effectively the case by projecting the pressure field on the normal modes of the system and determining the evolution of the modal amplitude. The model is formulated in section 3.1. The coupling term is then used in section 3.2 to see if it can drive instabilities and to define the ranges of delays which can lead to instability.

2. Multi injector combustor experiments

Experiments are carried out on a multiple injector combustor (MIC) on the Mascotte test bench operated by ONERA. The MIC backplane geometry takes into account the key parameters in multiple flame combustion. The distance between the injector elements has been minimized to increase interaction effects. Dimensions of the chamber have been chosen to dissociate the eigenmodes and locate the first transverse eigenfrequency around 2 kHz with gaseous methane. The chamber (Fig.1) has a rectangular section. Dimensions are 35×25×5 cm^3. The upper and lower walls are respectively equipped with three and two cooled pressure transducers. The lateral side walls comprise transparent quartz windows (15×10 cm^2) allowing direct observation of the three flames in the visible and near UV range. The chamber ends with a sonic nozzle. The nozzle diameter is adjusted to reach the expected chamber pressure for the prescribed mass flow rates of oxygen and methane. In this experiment, the power density is not equal to that found in a practical devices but it is already sizable.

The modulation system is an essential element in this investigation. Combustion in the chamber is naturally stable. To observe combustion oscillations, the system has to be forced externally and a sufficient level of modulation is required to obtain an observable interaction with combustion. The modulator is first used to identify the eigenmodes under hot

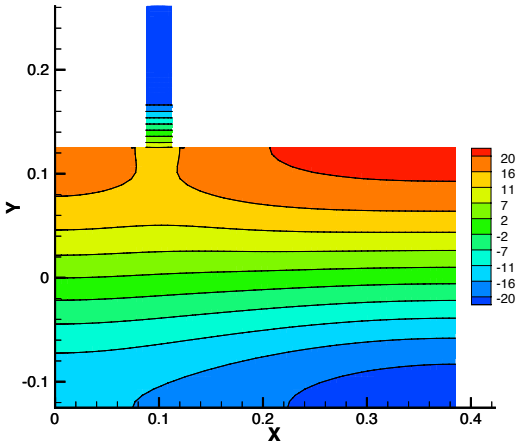

Figure 2: Structure of the first transverse acoustic mode in the combustion chamber calculated numerically for $\dot{m}_{LOx}/\dot{m}_{CH_4}$=0.6.

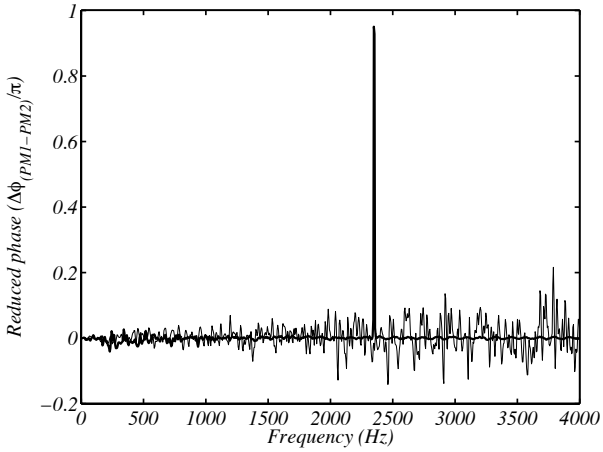

Figure 3: Non dimensional phase difference between the two PM without modulation (thin line) and with 2345 Hz modulated (bold line).

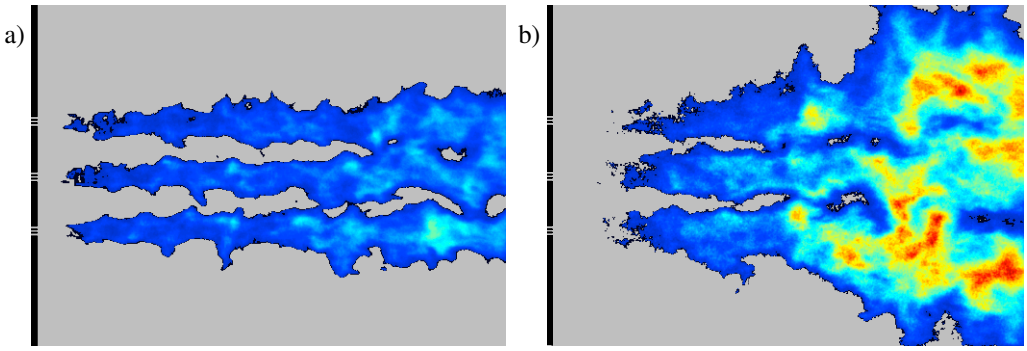

Figure 4: Instantaneous OH* emission (exposure time is $2\mu s$) without modulation (a) and with modulation at 2345 Hz (b) represented with the same intensity scale (arbitrary units)

fire conditions (by exciting the system at different frequencies and observing the resonance) and it is then exploited to excite the system at the first transverse eigenfrequency.
The modulator comprises an auxiliary nozzle placed on the top of the chamber (see Fig.1), at 100 mm from the injection plate. This forms a cylindrical cavity which crosses the top wall and ends with a sonic throat. The nozzle throat is periodically blocked by a rotating toothed wheel. The modulation frequency is adjusted with the rotation speed between 0 and 3500 Hz.

3D calculations are used to determine the eigenfrequencies and to illustrate the pressure distribution in the combustion chamber when the modulator is activated. Simulations are based on a finite element method discretizating the Helmholtz equation together with homogeneous boundary conditions such as a null acoustic pressure or a null acoustic normal velocity. The mesh includes the chamber and the secondary nozzle. The boundaries are treated as rigid walls with null velocity. The temperature is considered to be uniform and equal to the adiabatic one. The calculated frequencies proved to be close to what observed experimentally and the pressure distribution corresponding to the first transverse mode is plotted in Fig.2 for one value of the mixture ratio ($E = \dot{m}_{LOx}/\dot{m}_{CH_4} = 0.6$).

When modulated at the first transverse frequency, the pressure amplitude oscillation reaches 7% of the average chamber pressure which is significant enough to induce a strong coupling between acoustics and combustion (see Fig.4). This coupling manifests itself as a visible enhancement of flame spread and radiation from the flame is augmented by a large factor. The OH* emission intensity which can be linked to the heat release rate increases significantly.

The heat release rate is characterized with two photomultipliers (PM). Their aperture are vertically aligned in front of the quartz window (see Fig.1) at the end of the observable part of the chamber where the flames interact strongly

with the acoustic modulation. A spatial filter is fitted on the PM to reduce the observable area. The first PM records the light emission in the top part of the chamber while the second, 60 mm below, detects light emitted from the lower part of the chamber. The cross spectral analysis of the signals delivered by the two PM provide the phase between the light emitted in the top part of the chamber and the light originating from the bottom part. Figure 3 shows this phase relation as a function of the frequency when the system is modulated at the first transverse eigenfrequency (2345 Hz). Photo-multipliers indicate that the most intense emission area in the chamber oscillates transversally at the modulation frequency. The phase between the two PM is almost equal to 180 ° at 2345 Hz. A phase analysis, carried out at that frequency, indicates that pressure and OH* emission have similar spatial distributions and oscillate in phase. This behavior has been observed with a high speed camera. Films also feature enhanced reactive vortices convected in the downstream direction at a lower frequency. These experiments and the associated results are more deeply described in Ref.4. The model presented in the next section is directly inspired by the oscillations of the heat release at the modulation frequency.

3. Heat release model based on the velocity gradient

3.1 Description of the model

To begin with, it is worth revisiting early experiments on high frequency instability and specifically that of Ref.5. The objective is to reinterpret what was observed and devise a model for velocity coupled heat release oscillations. The experiment was carried out on a 10-cm diameter 1-m long model scale rocket engine equipped with a slit. A video camera recorded the light intensity through the transverse slit placed in a section at 14 cm from the injection plane. Figure 5 presents the light observed when a 6 000 Hz transverse mode is set-up in the chamber. The experiment shows that the luminous zone moves across the chamber in a helical way. The oscillation in the chamber is coupled with the first transverse acoustic mode. Under these conditions, energy is released periodically in the upper and lower sides of the chamber. The frequency of positive excursions of heat release in the upper part of the chamber coincides with the oscillation frequency. This is also true for the lower part. When heat release perturbation is positive in the upper part, it is negative in the lower part. The situation is reversed at each half period.

It is then natural to infer that positive heat release fluctuations occur at the same frequency as the transverse velocity variations. During one half period, the velocity is oriented in the upper direction while during the second part of the period it is directed towards the lower side of the chamber. This idea can now be used to devise an analytical model. It is first worth recalling that the coupling model which is proposed in this section aims at showing how velocity fluctuations may give rise to heat release fluctuations which will in turn constitute acoustic sources feeding energy into the transverse mode and eventually leading to instability. The model is established in a simplified framework where the pressure field inside the chamber is governed by a wave equation:

$$\frac{1}{c^2}\frac{\partial^2 p_1}{\partial t^2} - \nabla^2 p_1 = \frac{\gamma - 1}{c^2}\frac{\partial q_1}{\partial t} \tag{1}$$

The right hand side features the nonsteady rate of heat release $\partial q_1/\partial t$. The central issue is to express this term as a function of perturbations in the chamber. One may infer from the reexamination of Ref.5 and from experimental results obtained in the recent tests reported in Ref.4 that the rate of heat release term follows the acoustic velocity in the transverse direction. It will be assumed for simplicity that this term is proportional to this velocity. Very large velocity fluctuations directed upwards will lead to an accumulation of reactants in the upper part of the chamber. These reactants will burn at a later instant in time. Similarly large excursions of velocity in the negative direction will bring reactants in the lower part of the chamber and these will burn again after a certain delay.
It is then assumed that the nonsteady heat release term is proportional to the transverse velocity perturbation but it is important to include a delay τ in order to take into account time lag between the energy release and the wave oscillation. Thus the heat release is proportional to $v_1(y, t - \tau)$.

Based on the photograph in Fig.5, the heat release location in the chamber may be assumed to be correlated with the velocity direction. At an instant in time where the transverse component of velocity is positive in a cross section, reactants are displaced towards the top side of the chamber and the heat release will take place in that region. This will also induce a reduction of reactants in the lower side and consequently a negative fluctuation in heat release. Inversely, when the transverse component of the velocity is negative, the heat release will become positive in the lower part of the chamber and negative in the upper side. Consequently the sign of the heat release has to depend on the sign of the gradient of the transverse velocity:

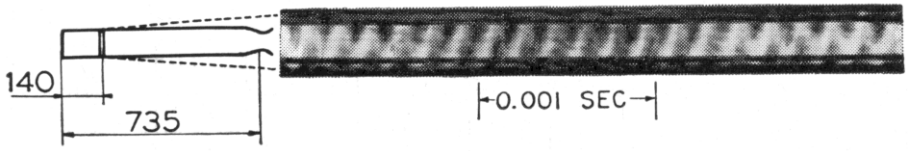

Figure 5: Streak film of a spiral mode of oscillation observed through a slit located at 14 cm from the injection plane. The oscillation frequency is 6000 Hz. (from Ref.5)

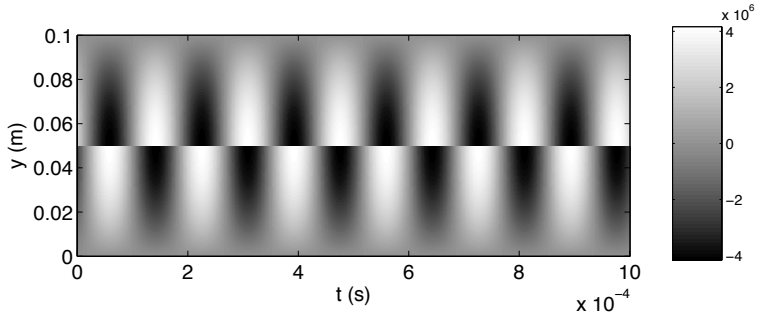

Figure 6: Time evolution of nonsteady heat release represented as a streak film taken through a transverse slit through a rectangular 2D combustor.

$$\frac{\partial q_1}{\partial t} = \beta \,\mathrm{sign}\left[\frac{\partial v_1}{\partial y}(y, t-\tau)\right] v_1(y, t-\tau) \tag{2}$$

In the previous expression β designates an interaction index.
The pressure in the chamber can be approximated by $p_1(y,t) = A(t)\cos(ky)\cos(\omega t + \phi)$ where A and ϕ are slowly varying functions of time. The transverse velocity v_1 is obtained from momentum equation

$$\rho_0 \frac{\partial v_1}{\partial t} + \frac{\partial p_1}{\partial y} = 0 \tag{3}$$

Using Eq.2 and 3 and the expression of $p_1(t)$, one may determine an analytical expression of the heat release. It is interesting to see how this compares with the experiments of Ref.5. To simplify the calculation one may consider a 2D duct with the same dimensions as the cylindrical chamber used in Ref.5 where a 6 000 Hz transverse acoustical mode is set-up. Under these conditions, the evolution with respect to time of the heat release in a transverse section deduced from expression 2 is displayed in Fig.6.

The pattern obtained in this way is clearly similar to the data shown in Fig.5. When a 6 000 Hz transverse mode is set-up in the chamber, six periods are observed during 1 ms in both cases. The positive heat release takes place alternately in the upper and then in the lower part of the chamber, forming a sinusoidal space-time distribution. The analytical expression adopted for the heat release (Eq.2) renders the phenomenon observed experimentally and this gives confidence in the initial assumption about the space-time heat release model.

3.2 Analysis of velocity coupling

From hereon the analysis may be developed in a standard way. The objective is to determine how the pressure amplitude evolves in the chamber when the coupling model is used to describe the nonsteady rate of heat release.
For this, it is convenient to use an expansion in terms of eigenmodes

$$p_1 = p_0 \sum_{n=1}^{\infty} \eta_n(t)\Psi_n(x)$$

where Ψ_n are such that $\nabla^2\Psi_n + \left(\omega_n^2/c^2\right)\Psi_n = 0$ and $\eta_n(t)$ designates the amplitude of the n-th mode. The chamber has a transverse size a and the first transverse eigenmode has the form $\Psi_1(y) = \cos(ky)$ where $k = \pi/a$. Considering that the eigenmodes are orthogonal, Eq.1 can be written

$$\frac{d^2\eta_n}{dt^2} + \omega_n^2\eta_n = \frac{\gamma-1}{p_0\Lambda_n}\int \frac{\partial q_1}{\partial t}\Psi_n\, dV \tag{4}$$

where $\Lambda_n = \int \Psi_n^2\, dV$. From Eq.2 and after integration of the source term in Eq.4, one finds

$$\frac{d^2\eta_1}{dt^2} + \omega_1^2\eta_1 = \alpha\, A(t)\sin[\omega(t-\tau)+\phi(t)] \tag{5}$$

$$\eta_1(t) = A(t)\cos[\omega t + \phi(t)] \tag{6}$$

with $\alpha = 2\beta(\gamma-1)/(p_0\Lambda_1\rho_0\omega)$
To determine the pressure evolution in the chamber and obtain stability conditions, the amplitude $\eta_1(t)$ has to be evaluated from Eq.5 and 6. It is convenient to consider that the amplitude and phase vary on a time scale which is much smaller than the period of oscillation and examine the evolutions of $A(t)$ and $\phi(t)$ with respect to time. In this analysis, one applies the two time expansion methods or more precisely the averaging techniques which are extensively used to examine nonlinear oscillations.
Differentiation of Eq.6 gives

$$\frac{d\eta}{dt} = \dot{A}\cos(\omega t+\phi) - A\dot{\phi}\sin(\omega t+\phi) - A\omega\sin(\omega t+\phi)$$

It is standard to assume that $\dot{A}\cos(\omega t+\phi) - A\dot{\phi}\sin(\omega t+\phi) = 0$. A second differentiation of Eq.5 yields the following system

$$\begin{cases} \dot{A}\cos(\omega t+\phi) - A\dot{\phi}\sin(\omega t+\phi) = 0 \\ \dot{A}\sin(\omega t+\phi) + A\dot{\phi}\cos(\omega t+\phi) = -\frac{\alpha}{\omega}A\sin\left[\omega(t-\tau)+\phi\right] \end{cases}$$

Taking the average of the previous system over a period of oscillation yields a set of first order differential equations for $A(t)$ and $\phi(t)$

$$\begin{aligned} \dot{\phi} &= \frac{\alpha}{2\omega}\sin(\omega\tau) \\ \frac{dA}{dt} &= -\frac{\alpha}{2\omega}\cos(\omega\tau)A(t) \end{aligned} \tag{7}$$

One may then deduce the pressure amplitude :

$$\eta_1(t) = B\,\exp\left(-\frac{\alpha}{2\omega}\cos(\omega\tau)t\right)\cos\left(\omega t + \frac{\alpha}{2\omega}\sin(\omega\tau)t\right) \tag{8}$$

Stability is easily deduced from Eq.7 which determines the evolution of the amplitude of oscillation with respect to time. The rate of growth will be positive if $\cos(\omega\tau) < 0$ or equivalently if $\omega\tau \in [\pi/2; 3\pi/2]$ modulo 2π. The system will then be unstable. This last situation is illustrated in Fig.7, where the first transverse mode is set-up at 3 330 Hz (close to the oscillation frequency of Ref.4), and $\omega\tau$ is equal to π. It is also possible to confirm this result by combining Eq.6 and Eq.5 to obtain a differential delayed equation

$$\frac{d^2\eta_1(t)}{dt^2} + \frac{\alpha}{\omega}\frac{d\eta_1(t-\tau)}{dt} + \omega^2\eta_1(t) = 0 \tag{9}$$

This equation can then be solved numerically. The calculation is carried out in a configuration similar to the present experiment. The pressure evolves as predicted in the analytical treatment (see Fig.7).

The model devised in this article clearly shows that a velocity coupling is possible. This takes however a somewhat unusual form because it depends on the delayed transverse velocity perturbations and on the sign of the gradient of this velocity. This last dependence reflects the physical phenomenon by which reactants are accumulated alternately in one side or in the other side of the chamber. The model provides a nonsteady rate of heat release which is similar to that observed in some early experiments of combustion instability in liquid rocket engines and it has been verified analytically and numerically that it can lead to an unstable growth of oscillations for certain ranges of delays.

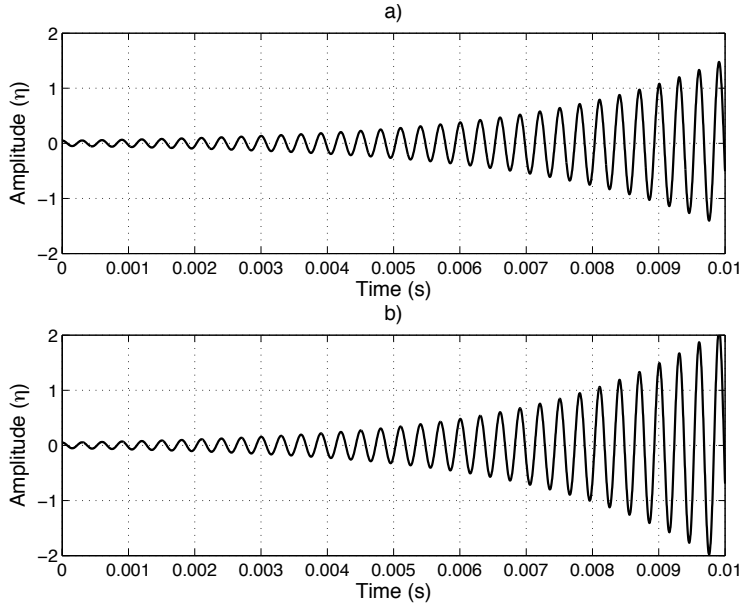

Figure 7: Pressure signal deduced from the velocity coupled model. The signal is plotted as a function of time for $\omega\tau = \pi$: (a) numerical solution, (b) analytical solution.

4. Conclusion

This article describes an analytical model for combustion instability involving velocity coupling. The model relies on a novel expression for the nonsteady rate of heat release. The heat release perturbation follows the delayed transverse velocity perturbation and the sign of the gradient of this velocity. Considering a rectangular chamber geometry similar to that of a multiple injector combustor, it is shown that the resulting heat release distribution can be subdivided in two regions separated by the symmetry axis. When the heat release perturbation is positive in the upper part of the chamber, it is negative in its lower part. This configuration is reversed after one half period. This sequential flipping of the heat release distribution corresponds to what is observed experimentally. It takes a shape which has some similarity with that of the pressure associated with the first transverse mode.

This model is explored analytically and numerically and it is shown that it can lead to an unstable growth of oscillations for finite ranges of the delay parameter. It will be generalized to cylindrical configurations in a near future, to be more precisely compared to Ref.5. The interaction index and the associated delay will also be modelled, using physical parameters.

This work was supported by Snecma, CNES and CNRS. The help of the Mascotte team of Onera is gratefully acknowledged.

References

[1] L. Crocco, J. Grey, and D. T. Harrje. On the importance of the sensitive time lag in longitudinal high-frequency rocket combustion instability. *Jet Propulsion*, 28(12):841–843, 1958.

[2] F. E. Culick and V. Yang. *Liquid Rocket Engine Combustion Instability*, volume 169, chapter Overview of Combustion Instabilities in Liquid-Propellant Rocket Engines, pages 3–37. AIAA, Inc, Washington, DC, 1995.

[3] J. C. Oefelein and V. Yang. Comprehensive review of liquid-propellant combustion instabilities in F1 engines. *Journal of Propulsion and Power*, 9(5):657–677, 1993.

[4] F. Richecoeur, P. Scouflaire, S. Ducruix, and S. Candel. High frequency transverse acoustic coupling in a multiple injector cryogenic combustor. *Journal of Propulsion and Power*, 22(4):790–799, 2006.

[5] A. O. Tischler and T. Male. Oscillatory combustion in rocket-propulsion engines. *Gas Dynamics Symposium*, pages 71–81, 1956.

[6] V. Yang, J. Wicker, and M. Yoon. *Liquid Rocket Engine Combustion Instability*, volume 169, chapter Acoustic Waves in Combustion Chambers, pages 345–355. AIAA, Washington, DC, 1995.

This page has been purposedly left blank